ISBN: 978-3-95450-248-6 ISSN: 2673-5490 doi: 10.18429/JACoW-IPAC2025-MOPM078

AUTOMATION OF PULSE IDENTIFICATION AT J-PARC*

S. Wagner†, H. Podlech[1], Institute of Applied Physics (IAP), Frankfurt, Germany
Y. Liu, KEK, Tsukuba, Japan
[1]also at Helmholtz Research Academy Hesse for Fair (HFHF), GSI Helmholtzzentrum für Schwerionenforschung, Campus Frankfurt, Frankfurt, Germany

Abstract

At J-PARC, the 500 µs long macro-pulses generated by the LINAC are separated into intermediate-pulses to synchronize it to the frequency of the Rapid-Cycling-Synchrotron (RCS). To secure a stable operation, the knowledge of position and length of those intermediate pulses are crucial, as the pulses need to be adjusted to the RCS frequency. The measurement for this adjustment is done by a beam position monitor (BPM), positioned directly behind the LINAC section in the low energy beam transport (LEBT) section. Since the form of the detected pulses can vary, the implementation of classical algorithms for the automatic detection and identification of pulses proved unreliable. Because of that, it was decided to develop a machine learning algorithm for the automatic pulse identification. In this paper, the background, training and results of different machine learning algorithms developed for the described problem will be introduced and discussed. Additionally, a test of the developed program during active beam operation is being planned, and will be introduced.

BACKGROUND

In this chapter, the linear accelerator as implemented at J-PARC shall be introduced, as well as the problem further discussed.

Linear Accelerator

The linear accelerator used by J-PARC accelerates 50 mA H^- ions from 50 keV up to 400 MeV. It consists of three normal conducting cavities of the Alvarez type and 30 normal conducting cavities of the separate-type DTL (SDTL). Additionally, a single annular coupled structure (ACS) was added to the LINAC during the energy upgrade. The working frequency is 324 MHz in the beginning (Alvarez-type and SDTL-type cavities) and 972 MHz in the end (ACS-type cavity). The repetition rate is either 25 Hz or 50 Hz, resulting in a duty cycle of 1.25 % to 2.5 % [1].

Which duty-cycle is used depends on the status of the planned transmutation experiment. If the experiment is running, the linear accelerator will be operated with a repetition rate of 50 Hz to feed both the transmutation experiment and the Rapid Cycling Synchrotron (RCS) with a frequency of 25 Hz each. At the current state, most of the time the LINAC is driven in the 25 Hz operation. The peak current of the used beam is 50 mA.

* Work supported by DAAD Germany
† s.wagner@iap.uni-frankfurt.de

Chopping of the Beam

In the end-section of the LINAC, before the beam is injected into the RCS (Fig. 1), the beam is chopped by two 324 MHz Radio-Frequency Deflection cavities [2]. Those choppers split the 500 µs long macro-pulse into roughly 500 ns long intermediate pulses. Those have to be synchronized with the RCS, which makes exact tracking of the intermediate pulses mandatory. This is done by a beam position monitor (BPM) which is located in the mid energy beam transport line of the LINAC.

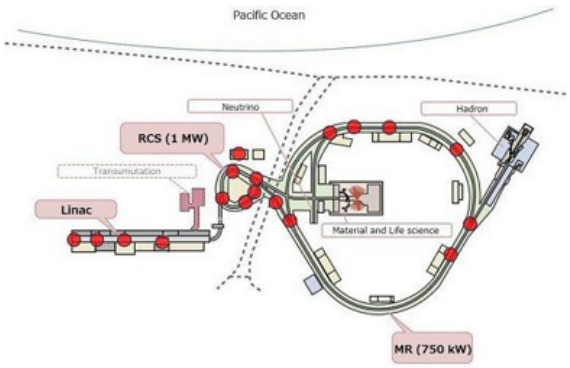

Figure 1: Schematic of the J-PARC accelerator [3].

After the chopping, the pulse can be distinguished into the macro-pulse and the intermediate pulse. The macro-pulse corresponds to the 500 µs pulse originating from the LINAC. It can be described as the original pulse, which will be modified by the chopper. After the chopper, the macro-pulse isn't continuous anymore, but is cut into smaller fragments as is described in Fig. 2.

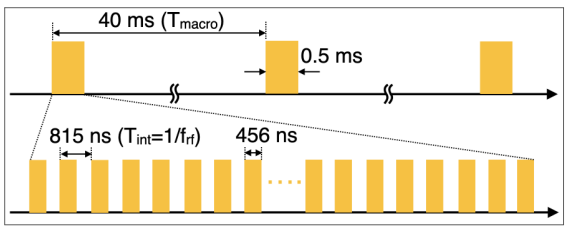

Figure 2: Transformation of the beam through the chopper. In (a), the macro-pulse (upper half) is magnified in the lower half to make the intermediate pulses visible [4].

BPM Monitor

During the energy upgrade of the J-PARC linac, the measuring setup was updated and increased, which involved

ISBN: 978-3-95450-248-6 ISSN: 2673-5490 doi: 10.18429/JACoW-IPAC2025-MOPM078

work on several BPMs in the LINAC section [5]. Those BPMs are of the stripline type and have high requirements regarding resolution. The BPM in question measures the x- and y-position of the beam, and then calculates the difference between those two signals. The resulting voltage is further transferred to the operating system, where it can be visualized and further analyzed. Depending on the position of the beam inside the BPM, three different shapes can emerge for the signal, which are further visualized in Fig. 3. Although two of the three possibilities are clearly marked with a strong positive or negative swing, the identification of the third possibility is more difficult. When the transmitted voltages nearly cancel each other out, the pulse is marked with a strongly suppressed background, resulting in a nearly flat curve. Due to the similarity between the background and this flat curve, the identification with classical algorithms proved difficult.

Since the pulse from the LINAC must be synchronized with the RCS, detailed knowledge of the pulse-form and position is mandatory. Even though the shape and position remain stable for most of the time, after maintenance and at the start of each shift, the LINAC pulses and the RCS have to be checked and synchronized. So far, this has been done manually, by examining the pulse shape and deriving the pulse length and position from the displayed data.

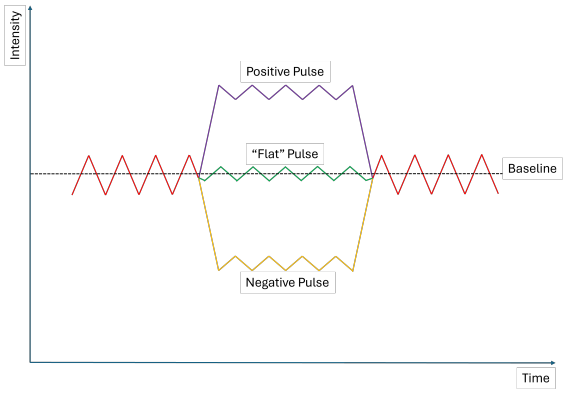

Figure 3: Examples of different pulse forms registered by the BPM monitor. The background is marked in red, while the pulses are marked in purple, green or yellow, in dependence of the type of pulse they are.

A possible solution would be to implement additional hardware with FPGAs or to separate the electronics for each electrode. However, since those would come with a significant investment cost, it was decided to first try machine learning algorithms to solve the existing problem with the available infrastructure.

MACHINE LEARNING BACKGROUND AND DEVELOPMENT PROCESS

Several different machine learning codes were tested during the development process of the introduced code. All of them were deep learning algorithms, which in the end proved to deliver good and reproducible results.

Deep Learning Algorithms

Deep learning algorithms consist of several layers. The first is the visible input layer. It feeds the input data into the network and has therefore strict restrictions when it comes to its dimensions. After the input layer, several hidden layers are stacked on one another. In those, the data is further processed and the weights of the hidden nodes of the layers are adjusted. The last layer is the output layer. It is again visible, and has as an output the desired information. During the training of a supervised machine learning algorithm, the output of this layer is compared with the true values of the labelled data to correct and adjust the weights of the network.

labeled Data

One of the most crucial parts in developing a machine learning algorithm is the preparation of the training data, with the labelling as one of the most important steps. Most of the time, it has to be done manually, as if classical algorithms would be able to label the data, a machine learning algorithm would not be needed. Due to the long runtime of the J-PARC accelerator, vast amounts of data from the BPM monitor in question are available. Those include all three different shapes of intermediate pulses in nearly the same quantity, making them ideal for training machine learning algorithms. The training set consisted of over 150 pulses, resulting in several hundred thousand up to over five million data points being used for training and testing. Since the algorithm learns from the labeled data, its quality is also of great concern. Every faultily labeled data point hinders the learning of the network, and since for the evaluation the results calculated by the network are compared to the labeled data, wrong labeled data points also compromise this compensation.

Training Results

The important parameter used for the evaluation is the accuracy. This value is calculated for the test data by calculating the percentage of correctly classified data points, which means that the prediction of the network was the same as the given label. Since the labelling was performed manually, the accuracy must be carefully evaluated. Some points may be wrongly labeled but rightly classified by the algorithm. This would then be evaluated as an incorrectly classified point.

Algorithms

All trained models were deep neural networks consisting of up to ten layers. Their general structure, as outlined in *Deep Learning Algorithms*, includes an input layer, multiple hidden layers, and an output layer for classification. The available data was divided into training and test data, with roughly 80 % training data and 20 % test data.

Convolutional Neural Network Convolutional Neural Networks (CNNs) are most known for their ability to identify images but can be applied to any problem where local feature identification is relevant. They use convolutional layers, in which small filters (kernels) slide across the input

ISBN: 978-3-95450-248-6 ISSN: 2673-5490 doi: 10.18429/JACoW-IPAC2025-MOPM078

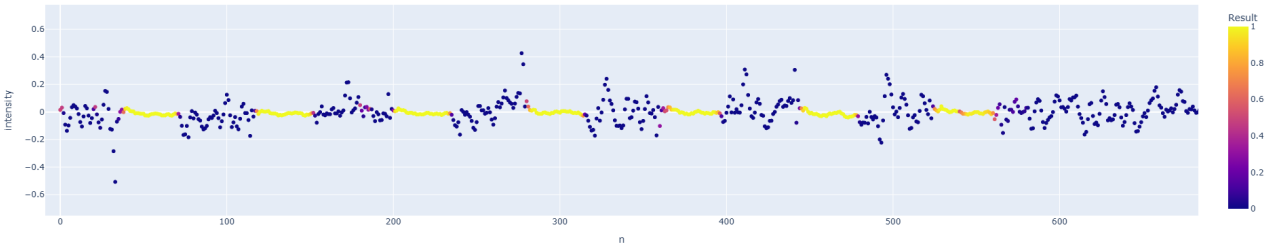

Figure 4: The certainty of a CNN-LSTM. Yellow points correspond with a high certainty for pulse, blue ones with a high certainty for background.

data and compute feature maps by applying element-wise multiplications followed by summation. The adjustable parameters include the number of different kernels, as well as their size and the activation function used after convolution.

Recurrent Neural Network Recurrent Neural Networks (RNNs) were developed to work with intrinsically structured data. Inside an RNN-cell the data of time step t_x is concatenated with the results for time step t_{x-1} and run through an activation function. The output of this cell is then combined with the data of time step t_{x+1} and put through the same mathematical operations and same weights as the previous data. It is also possible to combine CNNs and LSTMs (a subcategory of RNNs) to use the advantages of both model types.

Manual Corrections To further increase the accuracy of the models, manual corrections to filter out falsely identified points were implemented.

RESULTS AND EVALUATION

When the certainty of the network is plotted (compare Fig. 4) it is visible that the network is especially in the bordering regions of the pulse insecure. This can be explained by the higher error rate in border-areas of the pulse during labeling. Since the experimenter wasn't sure which point is the exact last one of the pulse, the network inherits this inaccuracy as well.

Out of the over 100 trained and tested networks, in the final configuration reached most of them over or near 95 % accuracy. The best performing network was an CNN-LSTM, whose final results are shown in Fig. 5. For the different configurations, which mostly differed in the number of layers and the length of input data given to them, the best network of each type is presented in Table 1.

SUMMARY AND ROADMAP

In this paper, the development process of a machine learning algorithm designed to identify intermediate pulses at the J-PARC LINAC was described. The final accuracies of most of the over hundred trained networks were comparable, and way above 95 %. For each tested category, the best accuracy were for the CNN-LSTM 97.16 %, for the CNN 97.12 % and for the LSTM 96.43 %.

Problematic regions in the border-region of the pulse were identified and can be explained by inherited behavior of the experimenter, e.g. uncertainties during labelling. Nonetheless, the training was deemed a success. As a next step, the code is planned to be implemented in June 2025 in the running system.

Table 1: Testing-Errors for Different Networks

Type	Input	Layers	Acc.
LSTM	800 ns	6	96.43 %
CNN	1500 ns	7	97.12 %
CNN-LSTM	1800 ns	4	97.16 %

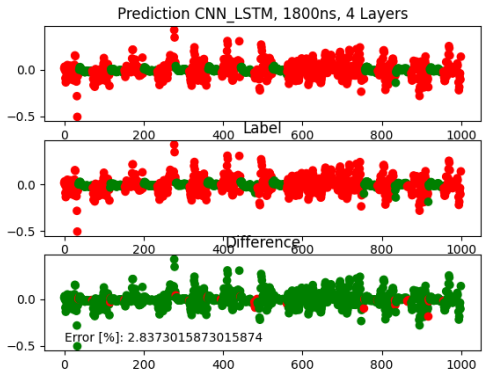

Figure 5: Examples of the results for a CNN-LSTM network. It was trained on 1800 ns long timesteps and consisted out of one CNN and four LSTM layers. Visible is the prediction (top), the label (middle) and the difference (bottom).

REFERENCES

[1] M. Ikegami, "Beam commissioning and operation of the J-PARC linac", *Prog. Theor. Exp. Phys.*, vol. 2012, no. 1, 2012. doi:10.1093/ptep/pts019

ISBN: 978-3-95450-248-6 ISSN: 2673-5490 doi: 10.18429/JACoW-IPAC2025-MOPM078

[2] M. Ikegami, A. Ueno, Y. Kondo, and T. Ohkawa, "A Simulation Study on Chopper Transient Effects in J-PARC Linac", in *Proc. LINAC'04*, Lübeck, Germany, Aug. 2004, paper TUP22, pp. 342–344.

[3] J-PARC-Center, JAEA and KEK Joint Project URL: https://j-parc.jp/public/Acc/en/index.html

[4] E. Cicek *et al.*, "Implementation of an Advanced MicroTCA.4-based Digitizer for Monitoring Comb-Like Beam at the J-PARC Linac", in *Proc. LINAC'22*, Liverpool, UK, Aug.-Sep. 2022, pp. 219–222. doi:10.18429/JACoW-LINAC2022-MOPORI02

[5] T. Miyao *et al.*, "'Beam Position Monitors for the ACS Section of the J-PARC Linac", in *Proc. DIPAC'11*, Hamburg, Germany, May 2011, paper TUPD18, pp. 341–343.

[6] Y. Fuwa, K. Moriya, and T. Takayanagi, "Design of Beam Focusing System with Permanent Magnet for J-PARC LINAC MEBT1", in *Proc. LINAC'22*, Liverpool, UK, Aug.-Sep. 2022, pp. 364–367. doi:10.18429/JACoW-LINAC2022-TUPOJO11